Separation Science and Technology
Publication details, including instructions for authors and subscription information:
http://www.informaworld.com/smpp/title~content=t713708471

Electrokinetic Properties of Vermiculite and Expanded Vermiculite: Effects of pH, Clay Concentration and Mono- and Multivalent Electrolytes

Osman Duman[a]; Sibel Tunç[b]
[a] Faculty of Education, Akdeniz University, Antalya, Turkey [b] Faculty of Arts and Sciences, Department of Chemistry, Akdeniz University, Antalya, Turkey

To cite this Article Duman, Osman and Tunç, Sibel(2008) 'Electrokinetic Properties of Vermiculite and Expanded Vermiculite: Effects of pH, Clay Concentration and Mono- and Multivalent Electrolytes', Separation Science and Technology, 43: 14, 3755 — 3776

To link to this Article: DOI: 10.1080/01496390802219109

URL: http://dx.doi.org/10.1080/01496390802219109

Separation Science and Technology, 43: 3755–3776, 2008

ISSN: 0149-6395 print/1520-5754 online
DOI: 10.1080/01496390802219109

Taylor & Francis
Taylor & Francis Group

Electrokinetic Properties of Vermiculite and Expanded Vermiculite: Effects of pH, Clay Concentration and Mono- and Multivalent Electrolytes

Osman Duman[1] **and Sibel Tunç**[2]
[1]Faculty of Education, Akdeniz University, Antalya, Turkey
[2]Faculty of Arts and Sciences, Department of Chemistry, Akdeniz University, Antalya, Turkey

Abstract: In this study, the zeta potential values of vermiculite and expanded vermiculite were measured to determine the effect of pH, clay concentration, and various mono- and multivalent electrolytes including NaCl, KCl, NH_4Cl, $NaNO_3$, $NaClO_4$, Na_2SO_4, Na_2CO_3, $Na_3PO_4 \cdot 12H_2O$, $MgCl_2 \cdot 6H_2O$, $CaCl_2 \cdot 2H_2O$, $BaCl_2$, $SrCl_2 \cdot 6H_2O$, $CuCl_2 \cdot 2H_2O$, $CoCl_2 \cdot 6H_2O$, $NiCl_2$, $AlCl_3$, and $CrCl_3 \cdot 6H_2O$ on the electrokinetic properties of vermiculite samples. It was found that generally the measured zeta potential values of expanded vermiculite for the studied systems were slightly more negative than that of vermiculite. The pH profiles of vermiculite and expanded vermiculite at acidic, natural, and basic pH values were obtained to determine the effect of time on the pH values of clay suspensions. The zeta potential measurements showed that the surface charge of clay particles was negative in water. The isoelectric point of vermiculite and expanded vermiculite were determined as pH 2.30 and 2.57, respectively. Divalent cations (Mg^{2+}, Ca^{2+}, Sr^{2+}, and Ba^{2+}), heavy metal ions (Cu^{2+}, Ni^{2+}, and Co^{2+}) and trivalent cations (Al^{3+} and Cr^{3+}) were potential determining ions for vermiculite and expanded vermiculite particles. Moreover, divalent and trivalent cations caused the change of surface charge from negative to positive. On the other hand, monovalent cations (Na^+, K^+ and $NH_4{}^+$), monovalent anions (Cl^-, $NO_3{}^-$, and $ClO_4{}^-$) and multivalent anions ($SO_4{}^{2-}$, $CO_3{}^{2-}$, and $PO_4{}^{3-}$) acted as indifferent ions for these clay particles.

Received 3 November 2007; accepted 15 April 2008.

Address correspondence to Sibel Tunç, Faculty of Arts and Sciences, Department of Chemistry, Akdeniz University, Antalya 07058, Turkey. Tel.: 90 242 310 23 24. Fax: 90 242 227 89 11. E-mail: stunc@akdeniz.edu.tr

Keywords: Electrokinetic properties, electrolyte solutions, expanded vermiculite, vermiculite, zeta potential

INTRODUCTION

Vermiculite is the mineralogical name given to hydrated laminar magnesium-aluminum-iron silicate. It is an expandable 2:1 mineral and often forms from alteration of mica (1,2). The structure of vermiculite is shown in Fig. 1. Its crystal lattice consists of one octahedral sheet sandwiched between two opposing tetrahedral sheets. A tetrahedral sheet is composed of corner-linked tetrahedra, whose central ions are Si^{4+} or Al^{3+}. The octahedral sheet is composed of edge-shared octahedra with Mg^{2+}, Al^{3+}, or Fe^{2+}. Due to isomorphic substitutions which are Al^{3+} for Si^{4+} substitution in tetrahedral layers and Mg^{2+} or Fe^{2+} for Al^{3+} substitution

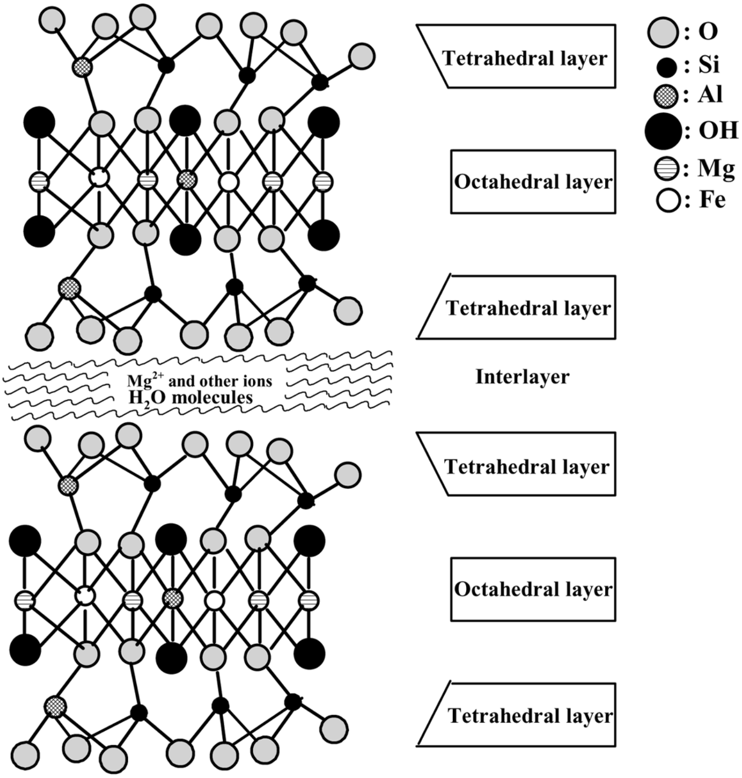

Figure 1. Structure of vermiculite.

in octahedral layers, vermiculite layers have permanent negative charges. These charges are compensated by the cations in the interlayer space (3–6). Moreover, vermiculite swells less than smectite due to its higher charge in the tetrahedral sheets and has higher elasticity and plasticity than kaolinite and mica (7).

If vermiculite is heated rapidly, it shows the unusual expanding property. When vermiculite is subjected to fast heating, its interlayer crystalline water transforms into steam and the pressure of steam forces the silicate layers apart from one another. As a result, expanded vermiculite with a large pore volume, a low bulk of density, and a high heat-insulating and sound-proof property is obtained (1,8).

Vermiculite is widely available, easily handled, odorless, and low-cost material. Due to their remarkable features, vermiculite and expanded vermiculite are widely used in agricultural (as fertilizer carrier, adsorbent, etc.), industrial (as fire protection, acoustic and thermal insulator, additive in concrete and plaster, packaging material, etc.), and environmental (as adsorbent) applications (9–11).

The electrokinetic properties of colloidal dispersions are great of importance in many industrial processes. The knowledge of electrokinetic properties of the colloidal particles is very important in obtaining the optimal conditions of a well-dispersed system in the clay/water suspensions (12). The isoelectric point value of clay particles and potential determining ions in the solution play a significant role in the adsorption of inorganic and organic species on the clay particles. They also govern the flotation, coagulation, and the dispersion properties in suspension systems (13,14).

It is known that zeta potential values of clay particles can change with solution pH and temperature, ionic strength, and type of ionic species in the solution. The sign and extent of zeta potential values are very valuable for industrial applications, especially in the flotation and adsorption processes (15,16).

Several studies have been performed to assess the adsorption behaviors of vermiculite. Abate and Masini (17) studied the adsorption of Cd^{2+} and Pb^{2+} onto vermiculite and they investigated the effect of pH, ionic strength, and humic acid on the adsorption properties of vermiculite. In another study, Abate et al. (18) reported the removal of fulvic acid from aqueous solution onto modified vermiculite. The adsorption behaviors of some heavy metal ions such as Mn^{2+}, Ni^{2+}, Zn^{2+}, Cd^{2+}, Cu^{2+}, and Pb^{2+} onto vermiculite were investigated by Malandrino et al. (7) and they concluded that the metal uptake on the clay was hindered by the presence of strong complexing agents. The efficiency of vermiculite as an adsorbent was also tested to remove of some of the heavy metal ions from aqueous solutions (19–21).

The electrokinetic properties of various clays such as clinoptilolite (22), kaolinite (23,24), perlite (25,26), sepiolite (14), imogolite (27), and bentonite (28,29) in the presence of different electrolytes or molecules were studied previously, but there was not any research related with vermiculite and expanded vermiculite in the literature.

The aim of the present study was to investigate the effect of some mono- and multivalent salts including NaCl, KCl, NH_4Cl, $NaNO_3$, $NaClO_4$, Na_2SO_4, Na_2CO_3, $Na_3PO_4 \cdot 12H_2O$, $CuCl_2 \cdot 2H_2O$, $CoCl_2 \cdot 6H_2O$, $NiCl_2$, $MgCl_2 \cdot 6H_2O$, $CaCl_2 \cdot 2H_2O$, $BaCl_2$, $SrCl_2 \cdot 6H_2O$, $AlCl_3$ and $CrCl_3 \cdot 6H_2O$ on the electrokinetic behaviors of vermiculite and expanded vermiculite particles. The examination of the effect of clay concentration, pH, ionic species and electrolyte concentration on the zeta potential was also aimed.

MATERIALS AND METHODS

Materials

Vermiculite sample was supplied from Shanghai, China. To prepare the expanded vermiculite, firstly, vermiculite was placed in a furnace heated to 500°C. Then, the sample was kept at this temperature for 1–2 s and taken out of the furnace. The obtained sample was labeled as expanded vermiculite.

NaCl, KCl, and $NaClO_4$ were purchased from Sigma, NH_4Cl, $CuCl_2 \cdot 2H_2O$, $MgCl_2 \cdot 6H_2O$, $CaCl_2 \cdot 2H_2O$, $SrCl_2 \cdot 6H_2O$, $CrCl_3 \cdot 6H_2O$, $CoCl_2 \cdot 6H_2O$, and Na_2CO_3 from Merck, and $BaCl_2$, $NiCl_2$, $AlCl_3$, $NaNO_3$, Na_2SO_4, and $Na_3PO_4 \cdot 12H_2O$ from Aldrich. All other chemicals were reagent grade. Deionized water was used in all experiments.

Methods

Purification of Vermiculite and Expanded Vermiculite

Vermiculite and expanded vermiculite samples were purified before using in the experiments. A suspension was obtained by adding of 100 g clay sample into 1 L deionized water to prepare the purified samples. This suspension was stirred at 960 rpm for 24 h by Variomag Poly model magnetic stirrer. Then the suspension was filtered through filter paper (filter diameter: 125 mm). Purified samples were dried at 110°C for 24 h. Dried samples were blended using a Waring Commercial Blendor for 5 min at high speed (30). After then samples were sieved by 100 µm sieve. The particles under 100 µm were used in the further experiments.

Characterization of Vermiculite Samples

X-ray diffraction (XRD) measurement of vermiculite sample was performed using a Shimadzu XRD-6000 model diffractometer. The XRD pattern of vermiculite shows that the sample consists of mainly vermiculite and small amounts of illite and hydrobiotite as impurities. Chemical compositions of vermiculite and expanded vermiculite were analyzed by X-ray fluorescence (XRF) spectrometer and results were presented in Table 1. As seen from Table 1, the chemical compositions of vermiculite and expanded vermiculite are similar. These samples are of essentially Si^{4+}, Mg^{2+}, Al^{3+}, Fe^{3+}, and K^{+}. X-ray measurements were carried out by the Scientific and Technological Research Council of Turkey (TUBITAK).

The cation exchange capacity (CEC) and the density values of vermiculite and expanded vermiculite were determined by ammonium acetate method and picnometric method, respectively.

A Zeiss Leo-1430 model scanning electron microscope (SEM) was used to observe the morphology of the vermiculite samples. SEM images of vermiculite and expanded vermiculite were shown in Fig. 2a and in Fig. 2b, respectively. It was seen from these figures that expanded vermiculite was more voluminous than vermiculite owing to vaporization of water from interlayers of vermiculite during the production of expanded vermiculite.

The specific surface area values of vermiculite samples were obtained from N_2 adsorption isotherms by Quantachrome Autosorb-1-C/MS. These values were calculated according to Brunauer-Emmett-Teller (B.E.T.) method (31) using the N_2 adsorption isotherm data. The specific surface area measurements were carried out by Central Laboratory of Middle East Technical University, Ankara, Turkey.

Table 1. Chemical composition of vermiculite samples

Compound	Vermiculite (%)	Expanded vermiculite (%)
Na_2O	0.8	0.8
MgO	28.8	29.1
Al_2O_3	12.0	12.2
SiO_2	36.9	37.0
K_2O	7.0	6.4
CaO	1.8	1.7
TiO_2	1.9	1.9
Fe_2O_3	10.0	10.1
BaO	0.5	0.5
Cr_2O_3	0.3	0.3

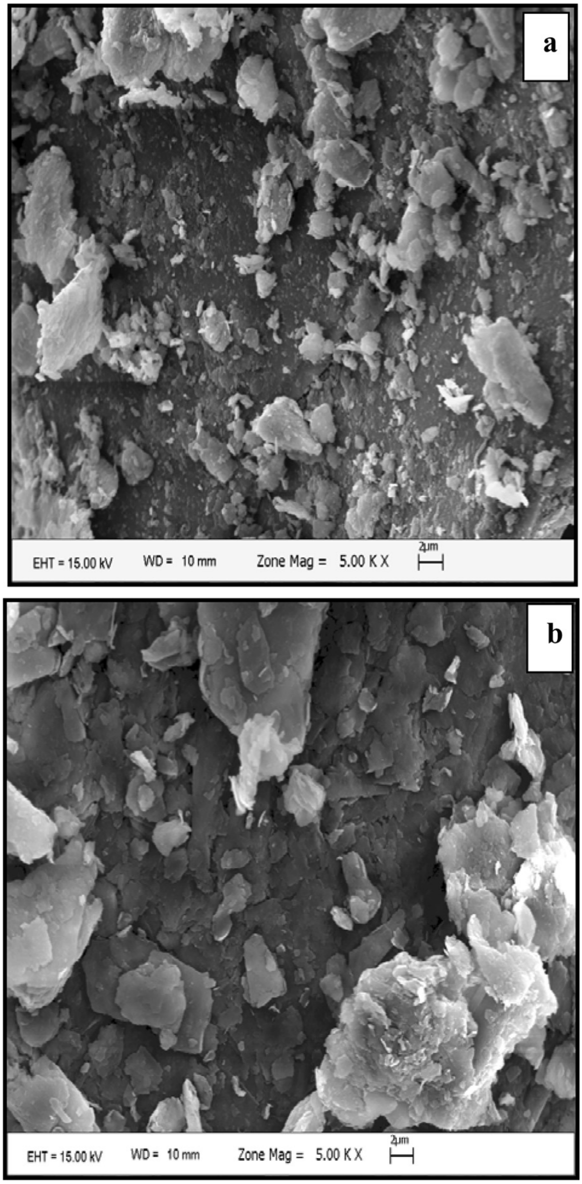

Figure 2. SEM images of vermiculite (a) and expanded vermiculite (b).

The obtained results from the CEC, density, and specific surface area measurements of vermiculite samples were given in Table 2. The CEC value was almost the same for vermiculite and expanded vermiculite.

Table 2. Physicochemical properties of vermiculite and expanded vermiculite

Sample	CEC (meq/100 g)	Density[a] (g/cm^3)	Specific surface area (m^2/g)
Vermiculite	56.04	2.894	7.8
Expanded vermiculite	56.84	0.400	9.8

[a] The values were obtained for the original samples.

On the other hand, the density of vermiculite decreased approximately 7-fold after the expansion process. The specific surface area value of expanded vermiculite was higher than that of vermiculite. This can be explained with the increase of pore volume or the decrease of density of expanded vermiculite due to vaporization of water from interlayer and silicate layers apart from one another.

The FTIR spectra of vermiculite samples were recorded by the KBr pellet technique. The KBr pellets were prepared by mixing clay samples with KBr powder (1:100) and using a mass of 10 tons. Tensor 27 model of FTIR (Bruker) was used to obtain the IR spectra of samples. FTIR spectra of vermiculite and expanded vermiculite recorded in the range of 400–4000 cm^{-1} at a resolution of 2 cm^{-1} is shown in Fig. 3. The FTIR spectra of vermiculite and expanded vermiculite are similar (Fig. 3). The O-H stretching vibration related to OH groups of interlayer water and the silanol groups is observed at 3717 cm^{-1} and 3418 cm^{-1}, respectively. The absorption band observed at 1640 cm^{-1} attributes to the characteristic bend deformation of the O-H group of water. The sharp peak at

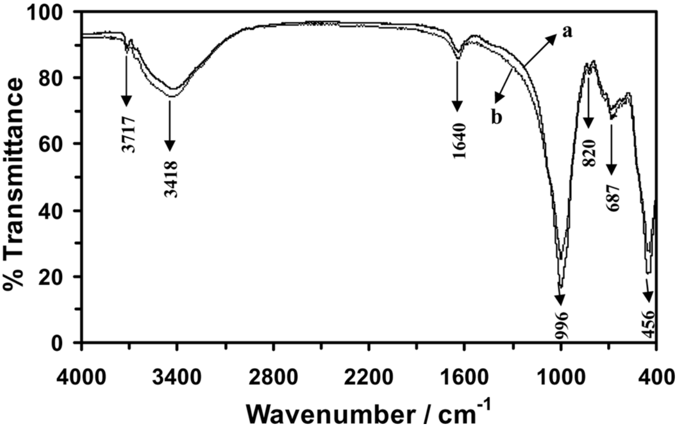

Figure 3. FTIR spectra of vermiculite (a) and expanded vermiculite (b) samples.

$996\,\mathrm{cm}^{-1}$ is assigned to the Si-O stretching vibration. The bending vibration of Al-OH appears at $820\,\mathrm{cm}^{-1}$. The Al-O bending vibration is observed at $687\,\mathrm{cm}^{-1}$. The peak at $456\,\mathrm{cm}^{-1}$ indicates the Si-O-Mg bending vibration (20,32,33).

Zeta Potential Measurements

Zeta potential measurements were carried out by Nano-ZS model (Malvern) zetasizer instrument. This instrument works with the technique of laser doppler electrophoresis (4 mW He-Ne, 633 nm). Electrophoretic mobilities (U_E) of particles were measured by the instrument and then automatically converted to zeta potential (ζ) by using Smoluchowski equation (Eq. (1)),

$$\zeta = \frac{4\pi\eta}{\varepsilon} U_E \tag{1}$$

where η is the viscosity of suspending liquid, ε is the dielectric constant of suspending liquid, and π is a constant (34).

Zeta potential measurements were performed to determine the effect of clay concentration, pH, ionic species, and electrolyte concentration on zeta potential.

A sample of 0.4 g clay in 100 mL deionized water containing desired electrolyte concentration was added to erlenmeyer and then mixed at 400 rpm for 24 h by Variomag Poly model of magnetic stirrer kept in Sanyo MIR-250 incubator at 25.0 ± 0.5°C. The equilibrium time was selected as 24 h for all experiments. The pH was adjusted by addition of HCl or NaOH solutions and measured with a glass combined electrode. The average of 15 measurements was used to represent the zeta potential data. The percentage difference in the measured zeta potential values of suspensions was, on the average, less than 4% of the mean of the 15 values.

RESULTS AND DISCUSSION

Effect of Clay Concentration on the Zeta Potential Values

Insufficient clay concentration in the suspension can cause some errors in the measurement of the zeta potential. For this reason, before the zeta potential measurement of clay/electrolyte suspensions, vermiculite, or expanded vermiculite, suspensions having different clay concentrations in water were prepared and their zeta potentials were measured.

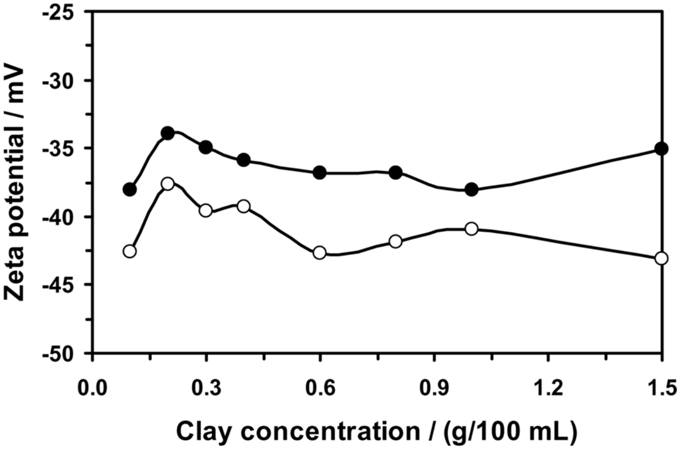

Figure 4. The variation of zeta potential of vermiculite (●) and expanded vermiculite (○) as a function of clay concentration.

The variation of zeta potential with clay concentration for vermiculite and expanded vermiculite were shown in Fig. 4. The zeta potential values of both vermiculite samples did not change significantly with increasing clay concentration. Therefore, in the subsequent zeta potential measurements, the vermiculite or expanded vermiculite to liquid ratio has been kept constant as 0.4 g/100 mL.

Moreover, the measured zeta potential values of both vermiculite and expanded vermiculite in water were negative in the studied clay concentration range of 0.10% and 1.5%. The reason of the negative charge may be the isomorphous substitution of Si^{4+} by Al^{3+} in the tetrahedral sheet and the broken bonds at the siloxane group of vermiculite samples (22,35). It should be noted that the zeta potential value of expanded vermiculite at the same clay content was lower than that of vermiculite. This may be due to an increase in the broken bond during the expansion process resulting in more negatively charge on the surface of expanded vermiculite.

Effect of pH on the Zeta Potential Values and Isoelectric Point (pH_{IEP})

Potential determining ions are responsible for the development of surface charge and surface potential. These ions control the surface reactions. Potential determining ions are generally H^+ and OH^- ions for the metal oxides or hydroxides (36). OH^- can be considered as an equivalent of a

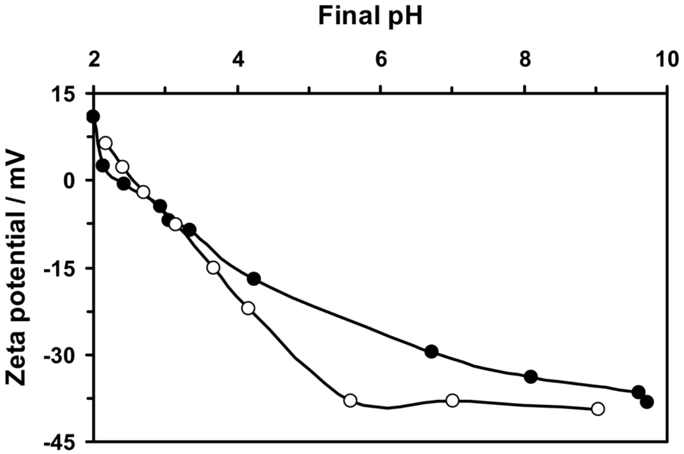

Figure 5. Zeta potential of vermiculite (●) and expanded vermiculite (○) as a function of pH.

lattice constituent ion and H^+ may replace with metallic cation (22). The measured zeta potentials at different equilibrium suspension pH values were shown in Fig. 5. It could be said that adsorption/desorption of H^+ or OH^- ions on the clay particle led to the formation of surface charge, thus these ions were potential determining ions for the vermiculite and expanded vermiculite particles.

The isoelectric point is a pH value at which the total amount of positive charge on the surface of solid is equal to the total amount of negative charge on it. The amount of net surface charge of solid or zeta potential value is zero at the isoelectric point. The isoelectric point is a characteristic property of solid particles and that is why it is important to know the isoelectric point of particles for the adsorption or flotation processes.

To determine the isoelectric point of clay samples, vermiculite, and expanded vermiculite suspensions (0.4 wt%) with different initial pH values were prepared by the addition of HCl or NaOH solution and they were mixed at 400 rpm for 24 h at 25.0 ± 0.5°C. Then, the final pH value and zeta potential value of each suspension were measured. The measured zeta potential values for each final pH value of suspensions were shown in Fig. 5. The obtained results indicated that the zeta potential values of vermiculite samples were positive in the low pH values. The increase of the suspension pH caused the negative surface charge. In the pH range of about 4 and 9, the zeta potential values of expanded vermiculite were lower than that of vermiculite. The isoelectric points of vermiculite and expanded vermiculite were determined as 2.30 and 2.57, respectively (Fig. 5).

The electrical charge at the oxide surface/aqueous phase on protonation or deprotonation of the surface hydroxyl can be ascribed as (14)

$$\text{▒-SOH} + H^+ \rightleftharpoons \text{▒-SOH}_2^+ \tag{2}$$

$$\text{▒-SOH} + OH^- \rightleftharpoons \text{▒-SO}^- + H_2O \tag{3}$$

and at the isoelectric point

$$[\text{▒-SOH}_2^+] = [\text{▒-SO}^-] \tag{4}$$

It can be said that the reaction in Eq. (2) and the reaction in Eq. (3) are responsible for the surface charge of vermiculite and expanded vermiculite particles below the isoelectric point and above the isoelectric point, respectively.

The sign of charges of the vermiculite particles at the edge sites under different pH values was given in the following equation (35)

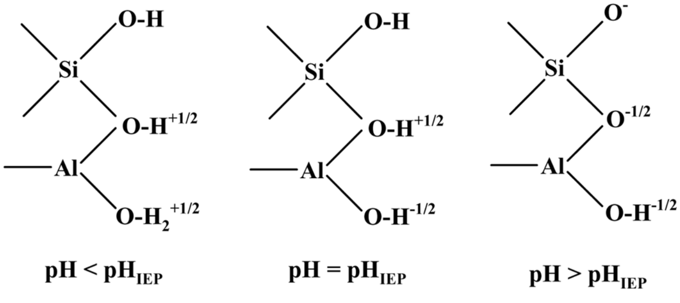

(5)

pH Profiles of Vermiculite and Expanded Vermiculite Suspensions

The knowledge of the pH change of a suspension with time is of great importance for the industrial and environmental applications. The stability of the clay suspension depends on the initial pH values of water before preparation of clay/water suspension. For this reason, the pH profiles of vermiculite and expanded vermiculite in a 0.4 wt% suspension as a function of time were obtained at acidic, natural and basic pH values. The pH profiles of the vermiculite samples were shown in Fig. 6.

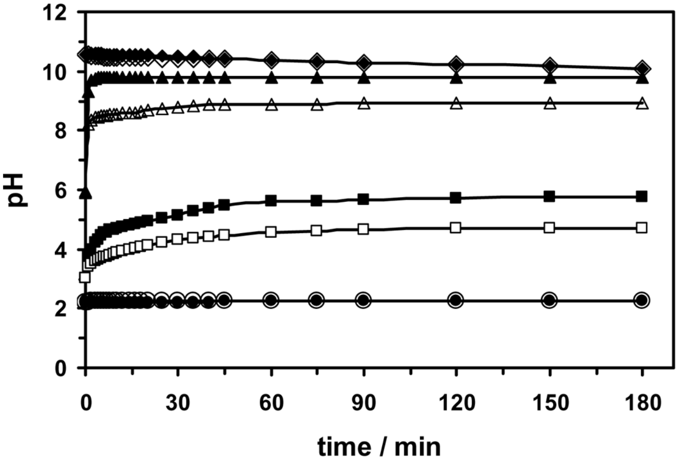

Figure 6. The variation in the pH values of vermiculite (initial pH values (●): 2.20; (■): 3.01; (▲): 5.95 and (◆): 10.58) and expanded vermiculite (initial pH values (○): 2.20; (□): 3.03; (△): 5.95 and (◆): 10.58) suspensions as a function of time.

In the first state, the initial pH value of water was adjusted to 2.20 by adding of HCl before preparation of clay/water suspension. Then, the clay was added on it and the pH value of the suspension was recorded at various time intervals. At the end of 180 min, the pH values of both vermiculite and expanded vermiculite suspensions were measured as 2.24. This showed that at the low pH value, the suspension pH value maintained its stability. In other words, the suspension pH value did not change significantly with time. This result can be explained with considering the surface charge at the edge sites of clay particles. Since the initial suspension pH values were approximately the same with pH_{IEP} ($pH \sim pH_{IEP}$ (Eq. (5)), H^+ or OH^- adsorption/desorption from the solution onto the surface of clay particles did not occur.

In the second state, the initial pH value of water was adjusted to about 3.0 by adding of HCl. After that the clay sample was mixed with water and the pH value of the suspension was measured. The pH values of vermiculite and expanded vermiculite suspensions increased from 3.01 to 5.77 and 3.03 to 4.71, respectively, at the end of 180 min. When the pH values of clay suspensions were compared, the change of pH in the vermiculite suspension was much higher than the change of pH in the expanded vermiculite suspension. The reason for the increase of suspension pH values with time was the adsorption of H^+ ions from solutions to the negatively charged surface of vermiculite or expanded vermiculite

($pH > pH_{IEP}$ (Eq. (5)). It should be noted that the adsorption of H^+ onto vermiculite more occurred than expanded vermiculite.

In the third state, vermiculite samples were added to the deionized water whose pH value was 5.95. The pH value of vermiculite suspension increased sharply within the first 5 min, after then it did not change until the end of 180 min. A similar increase was also observed for the expanded vermiculite suspensions, but its pH value was lower than that of the vermiculite suspension. After they were mixed for 180 min, the equilibrium suspension pH values of vermiculite and expanded vermiculite were measured as 9.79 and 8.93, respectively. Similar to the second state, the increases at the pH value of clay suspensions can be explained with the adsorption of H^+ ions from solution to the surface of clays (Eq. (5)).

In the fourth state, the initial pH value of water was adjusted to 10.58 by adding of NaOH. Then, the clay was added to the water and the pH change of suspension followed. After 180 min, a slight decrease was observed from 10.58 to 10.10 at the pH values of the clay suspensions. The transfer of the proton from $-SiOH$ (or $-AlOH$) groups in the lattice of vermiculite samples to free OH^- ions with forming H_2O in the suspension may cause a decrease in pH value.

Effects of Electrolytes on Zeta Potential of Vermiculite and Expanded Vermiculite

Effect of Monovalent Electrolytes

The variation of zeta potential of vermiculite and expanded vermiculite with monovalent cation concentration such as Na^+, K^+, and NH_4^+ and with monovalent anion concentration such as Cl^-, NO_3^-, and ClO_4^- were given in Fig. 7 and Fig. 8, respectively. A potential determining cation should make the surface more positive with an increased concentration of cation. Similarly, a potential determining anion should make the surface more negative with an increase in its concentration. The opposite sign ions with the solid surface accumulate near the solid surface and equilibrate the surface electrical charge. These ions accumulated at the solid/liquid interface are known as counterions. Counterions are adsorbed by Coulombic or electrostatic attraction at the solid surface bearing the potential determining ions. If the counterions are adsorbed by electrostatic attraction alone, their source in solution is called an indifferent ion (23).

According to the above definitions, monovalent cations such as Na^+, K^+, and NH_4^+ and monovalent anions such as Cl^-, NO_3^-, and ClO_4^-

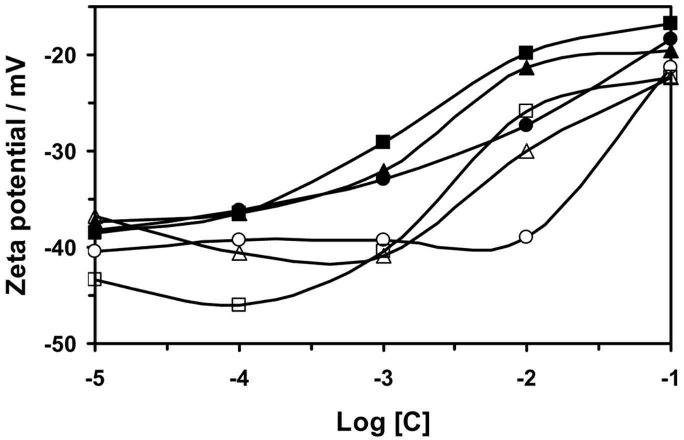

Figure 7. The variation of zeta potential of vermiculite (in the presence of (●): NaCl, (▲): KCl and (■): NH_4Cl) and expanded vermiculite (in the presence of (○): NaCl, (△): KCl and (□): NH_4Cl) samples with monovalent cation concentration.

were not potential determining ions for vermiculite and expanded vermiculite particles (Figs. 7 and 8). Similar observations were reported in the literature for monovalent electrolyte/sepiolite (14) and monovalent electrolyte/clinoptilolite (22) systems. These ions acted as indifferent ions

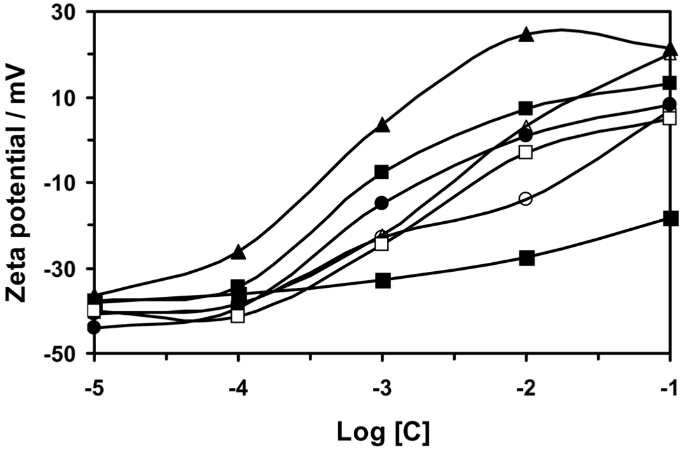

Figure 8. The variation of zeta potential of vermiculite (in the presence of (●): NaCl, (▲): $NaNO_3$ and (■): $NaClO_4$) and expanded vermiculite (in the presence of (○): NaCl, (△): $NaNO_3$ and (□): $NaClO_4$) samples with monovalent anion concentration.

and they only compressed the electrical double layer, because indifferent ions can only reduce the zeta potential asymptotically to zero (26).

For an aqueous solution of a symmetrical electrolyte at 25°C, the thickness of double layer, 1/K (m), is given by

$$\frac{1}{K} = \frac{1}{0.329 \times 10^{10}} \cdot \frac{1}{(C \cdot Z^2)^{1/2}} \tag{6}$$

where C is the ion concentration (M) and Z is the valency of ion. For unsymmetrical electrolytes, the thickness of the electrical double layer can be calculated by taking Z to be the counter-ion charge number (36). It is seen from Eq. (6) that the thickness of the diffused double layer depends on the ionic strength of the electrolyte and the valency of the ion. For a 1–1 electrolyte, the thickness of the double layer is 0.962 nm for a 1×10^{-1} M solution and 9.62 nm for a 1×10^{-3} M solution.

Moreover, the experimental data demonstrated that the zeta potential value for the vermiculite/monovalent electrolyte systems at the same electrolyte concentration was higher (less negative) than that of the expanded vermiculite/monovalent electrolyte systems (Figs. 7 and 8).

Effect of Divalent Electrolytes

The $MgCl_2 \cdot 6H_2O$, $CaCl_2 \cdot 2H_2O$, $SrCl_2 \cdot 6H_2O$, $BaCl_2$, Na_2SO_4, Na_2CO_3, $CuCl_2 \cdot 2H_2O$, $NiCl_2$, and $CoCl_2 \cdot 6H_2O$ were used in order to investigate the effects of various divalent electrolytes and heavy metal salts on the zeta potential values of vermiculite and expanded vermiculite. Figures 9, 10, and 11 show the variation of zeta potential of vermiculite samples in the presence of divalent cations such as Mg^{2+}, Ca^{2+}, Sr^{2+}, and Ba^{2+}, heavy metal ions such as Cu^{2+}, Ni^{2+}, and Co^{2+}, and divalent anions such as SO_4^{2-} and CO_3^{2-}, respectively.

As seen from Fig. 9 that the zeta potential values of both vermiculite and expanded vermiculite became less negative with increasing divalent cation concentration. The negative zeta potential values for these systems were converted to positive values at 1×10^{-1} M divalent cation concentration. Therefore, Mg^{2+}, Ca^{2+}, Sr^{2+}, and Ba^{2+} were potential determining cations for vermiculite and expanded vermiculite. These cations were specifically adsorbed in the Stern layer. In the presence of Mg^{2+}, Ca^{2+}, Sr^{2+}, and Ba^{2+} concentration of 1×10^{-1} M, the measured zeta potential values were +9.79, +6.00, +3.63, and +5.17 mV for vermiculite and +3.66, +0.705, +0.920, and +4.41 mV for expanded vermiculite, respectively.

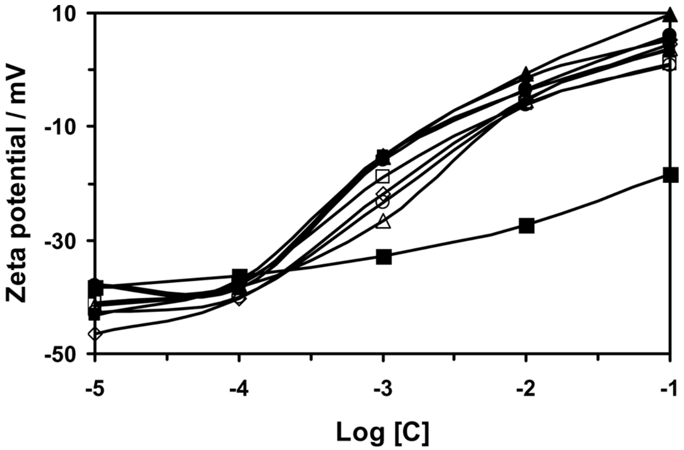

Figure 9. The variation of zeta potential of vermiculite (in the presence of (▲): $MgCl_2 \cdot 6H_2O$, (●): $CaCl_2 \cdot 2H_2O$, (■): $SrCl_2 \cdot 6H_2O$, (◆): $BaCl_2$, (■): NaCl) and expanded vermiculite (in the presence of (△): $MgCl_2 \cdot 6H_2O$, (○): $CaCl_2 \cdot 2H_2O$, (□): $SrCl_2 \cdot 6H_2O$, (◇): $BaCl_2$) samples with divalent cation concentration.

The zeta potential values of vermiculite and expanded vermiculite in the presence of heavy metal ions (Fig. 10) showed similar behaviors with clay/divalent cation systems. The change of zeta potential values from

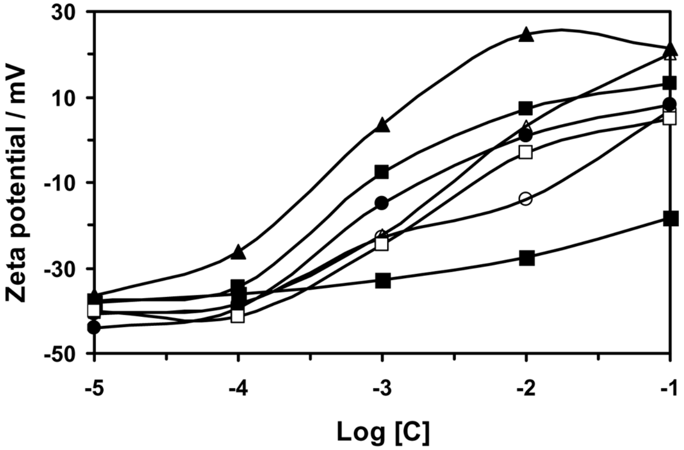

Figure 10. The variation of zeta potential of vermiculite (in the presence of (●): $CuCl_2 \cdot 2H_2O$, (▲): $NiCl_2$, (■): $CoCl_2 \cdot 6H_2O$, (■): NaCl) and expanded vermiculite (in the presence of (○):$CuCl_2 \cdot 2H_2O$, (△): $NiCl_2$, (□):$CoCl_2 \cdot 6H_2O$) samples with heavy metal ion concentration.

negative to positive appeared at the higher heavy metal ion concentrations than 1×10^{-2} M $CuCl_2 \cdot 2H_2O$ and $CoCl_2 \cdot 6H_2O$ and 1×10^{-3} M $NiCl_2$ for vermiculite. This change was observed in the presence of 1×10^{-1} M $CuCl_2 \cdot 2H_2O$, and $CoCl_2 \cdot 6H_2O$, and 1×10^{-2} M $NiCl_2$ for expanded vermiculite. The experimental results of the zeta potentials of clay/heavy metal ion systems showed that Cu^{2+}, Ni^{2+}, and Co^{2+} were also potential determining cations for the vermiculite samples.

When the sign of zeta potential values of clay samples was reversed (became positive), the suspension pH values of vermiculite and expanded vermiculite were measured as 4.41 and 3.33 for Cu^{2+}, 7.87 and 6.70 for Ni^{2+}, and 6.50 and 5.68 for Co^{2+}, respectively. In these pH values, heavy metal ions were non-hydroxyl forms (37). They can form hydroxyl complexes on the clay particles.

It should be noted that as the divalent cation concentration was increased, a decrease in the suspension pH values was observed for the studied divalent cation/clay systems. The first reason of this can be explained by the following reactions given by Davis et al. (38), (M^{2+} is a di-valent cation)

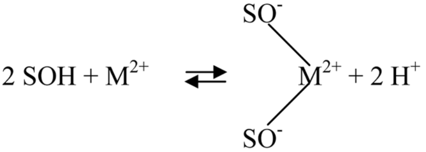

$$2\,SOH + M^{2+} \rightleftharpoons \begin{matrix} SO^- \\ \quad\diagdown \\ \quad\; M^{2+} + 2\,H^+ \\ \quad\diagup \\ SO^- \end{matrix} \tag{7}$$

$$SOH + M^{2+} + H_2O \rightleftharpoons SO^-\text{-}MOH^+ + 2\,H^+ \tag{8}$$

The second reason of decrease in the suspension pH values is the increase of divalent cation concentration.

The compression of the electrical double layer may also contribute to the decrease of the zeta potential values as the concentration increases. According to Eq. (6), divalent cations are more effective than monovalent cations for the compression of the electrical double layer and this may explain the trends in Figs. 9 and 10.

Based on the results shown in Fig. 11 for divalent anion/clay systems, it can be said that $SO_4{}^{2-}$ and $CO_3{}^{2-}$ were not potential determining anions, because the surface of the clay did not become more negative with increasing anion concentration. These anions could take place in the suspension as indifferent anions and they just contributed to the compression of the electrical double layer.

Effect of Trivalent Electrolytes

In Fig. 12, the zeta potential values of vermiculite and expanded vermiculite were plotted as a function of trivalent electrolyte concentration.

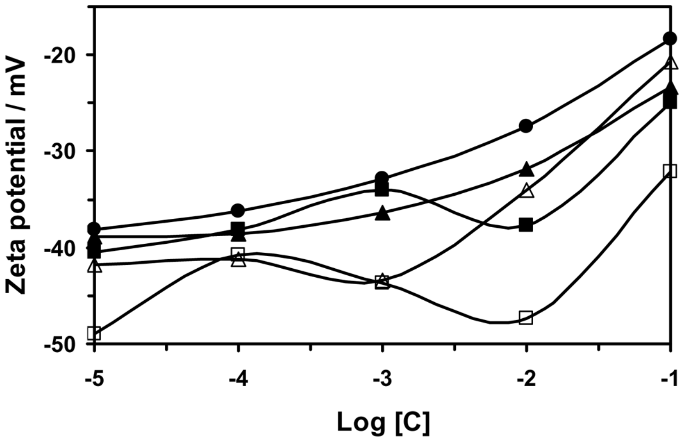

Figure 11. The variation of zeta potential of vermiculite (in the presence of (▲): Na_2SO_4, (■): Na_2CO_3, (●): NaCl) and expanded vermiculite (in the presence of (△): Na_2SO_4, (□): Na_2CO_3) samples with divalent anion concentration.

The trivalent cations, Al^{3+} and Cr^{3+}, were potential determining cations for the studied systems as divalent cations. On the other hand, the trivalent anion, PO_4^{3-}, was an indifferent anion and it only compressed the electrical double layer.

$AlCl_3$ and $CrCl_3 \cdot 6H_2O$ changed the surface charge of the vermiculite and expanded the vermiculite from negative to positive after the 1×10^{-3} M or higher trivalent ion concentration for vermiculite and the 1×10^{-2} M or higher trivalent ion concentration for the expanded vermiculite. This result can be explained again with the specific adsorption of Al^{3+} and Cr^{3+} ions onto the clay particles.

At the higher concentrations than 1×10^{-3} M at which the surface charge was reversed, the pH values of vermiculite/trivalent cation systems were in the range of 4.80 and 3.03 for Al^{3+} and 5.22 and 2.53 for Cr^{3+}. For the expanded vermiculite/trivalent cation systems in the trivalent electrolyte concentration range of 1×10^{-3} and 1×10^{-1} M, the pH values were measured between 4.39 and 2.70 for Al^{3+} and 5.00 and 2.05 for Cr^{3+}. In this case, Al^{3+} was in a non-hydroxyl form. On the other hand, Cr^{3+} was in various forms such as Cr^{3+}, $Cr(OH)^{2+}$, $Cr(OH)_2^{+}$, and $Cr_2(OH)_2^{4+}$ (20). These ions, Al^{3+} and Cr^{3+}, may form various hydroxy complexes with vermiculite and expanded vermiculite surfaces such as $Al(OH)_2^{+}$, $Al(OH)^{2+}$, $Al(OH)_3$, and $Cr(OH)_3$ (22,23).

When the zeta potential values of vermiculite and expanded vermiculite particles were compared in each trivalent electrolyte solution at the

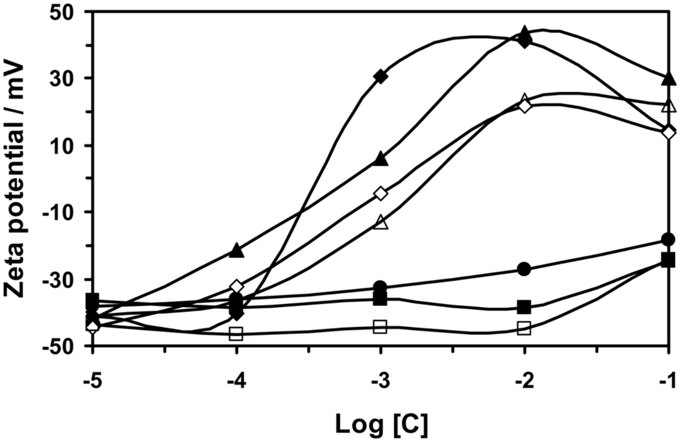

Figure 12. The variation of zeta potential of vermiculite (in the presence of (■): $AlCl_3$, (◆): $CrCl_3 \cdot 6H_2O$, (■): $Na_3PO_4 \cdot 12H_2O$, (●): NaCl) and expanded vermiculite (in the presence of (△): $AlCl_3$, (◆): $CrCl_3.6H_2O$, (□): $Na_3PO_4 \cdot 12H_2O$) samples with trivalent salts.

same concentration, it was seen that the zeta potential values of vermiculite were higher than that of the expanded vermiculite. Similar results were also observed for the monovalent and divalent electrolyte/clay systems.

CONCLUSIONS

The zeta potential values of vermiculite clays were negative in water. Clay concentration did not significantly affect the zeta potential values of vermiculite and the expanded vermiculite. The pH_{IEP} values of vermiculite and the expanded vermiculite were determined as pH 2.30 and 2.57, respectively. H^+ and OH^- ions were found to be potential determining ions for studied vermiculite clays. The pH profile of vermiculite and expanded vermiculite suspensions at acidic, basic, and natural pH values was obtained to determine the effect of time on the pH value of clay suspensions. It was concluded from the zeta potential measurements that monovalent cations (Na^+, K^+, and NH_4^+), monovalent anions (Cl^-, NO_3^- and ClO_4^-), divalent anions (SO_4^{2-} and CO_3^{2-}), and trivalent anions (PO_4^{3-}) were indifferent ions for the vermiculite clays and they only compressed the electrical double layer. However, divalent cations (Mg^{2+}, Ca^{2+}, Sr^{2+}, and Ba^{2+}), heavy metal ions (Cu^{2+}, Ni^{2+}, and Co^{2+}), and trivalent cations (Al^{3+} and Cr^{3+}) were potential determining cations. Divalent and trivalent cations reversed the sign of the surface charge from negative to positive.

ACKNOWLEDGEMENTS

The authors would like to thank the Management Unit of Scientific Research Projects of Akdeniz University for support of this work. The authors are grateful to Prof. Dr. Ertuğrul ARPAÇ for his permission to use Zetasizer and FTIR spectrometer instruments. The Central Laboratory of the Middle East Technical University and TUBITAK are acknowledged for determining some of the characterization properties of the vermiculite samples.

REFERENCES

1. Aristov, Y.I.; Restuccia, G.; Tokarev, M.M.; Buerger, H.D.; Freni, A. (2000) Selective water sorbents for multiple applications. 11. $CaCl_2$ confined to expanded vermiculite. *React. Kinet. Catal. Lett.*, *71*: 377.
2. Howe-Grant, M.. (1992) Kirk-Othmer Encyclopedia of Chemical Technology, 4th Ed., Vol. 6; John Wiley & Sons: New York.
3. Osman, M.A. (2006) Organo-vermiculites: synthesis, structure and properties. Platelike nanoparticles with high aspect ratio. *J. Mater. Chem.*, *16*: 3007.
4. Poyato, J.; Perez-Maqueda, L.A.; Justo, A.; Balek, V. (2002) Emanation thermal analysis of natural and chemically-modified vermiculite. *Clay. Clay. Miner.*, *50*: 791.
5. Tvardovski, A.V.; Fomkin, A.A.; Tarasevich, Y.I.; Polyakova, I.G.; Serpinski, V.V.; Guseva, I.M. (1994) Investigation of cation-substituted vermiculite deformation upon water vapor sorption. *J. Colloid Interf. Sci.*, *164*: 114.
6. Abollino, O.; Giacomino, A.; Malandrino, M.; Mentasti, E.. (2007) Interaction of metal ions with montmorillonite and vermiculite. *Appl. Clay Sci.* In press, doi: 10.1016/j.clay.2007.04.002.
7. Malandrino, M.; Abollino, O.; Giacomino, A.; Aceto, M.; Mentasti, E. (2006) Adsorption of heavy metals on vermiculite: Influence of pH and organic ligands. *J. Colloid Interf. Sci.*, *299*: 537.
8. Gordeeva, L.G.; Moroz, E.N.; Rudina, N.A.; Aristov, Y.I. (2002) Formation of porous vermiculite structure in the course of swelling. *Russ. J. Appl. Chem.*, *75*: 357.
9. Perez-Maqueda, L.A.; Caneo, O.B.; Poyato, J.; Perez-Rodriguez, J.L. (2001) Preparation and characterization of micron and submicron-sized vermiculite. *Phys. Chem. Minerals.*, *28*: 61.
10. Da Fonseca, M.G.; de Oliveira, M.M.; Arakaki, L.N.H.; Espinola, J.G.P.; Airoldi, C. (2005) Natural vermiculite as an exchanger support for heavy cations in aqueous solution. *J. Colloid Interf. Sci.*, *285*: 50.

11. Da Fonseca, M.G.; Cardoso, C.M.; Wanderley, A.F.; Arakaki, L.N.H.; Airoldi, C. (2006) Synthesis of modified vermiculite by interaction with aromatic heterocyclic amines. *J. Phys. Chem. Solids*, *67*: 1835.
12. Penner, D.; Lagaly, G. (2000) Influence of organic and inorganic salts on the coagulation of montmorillonite dispersions. *Clay. Clay. Miner.*, *48*: 246.
13. Somasundaran, P.; Fuerstenau, D.W. (1966) Mechanisms of alkyl sulfonate adsorption at the alumina-water interface. *J. Phys. Chem.*, *70*: 90.
14. Alkan, M.; Demirbaş, Ö.; Doğan, M. (2005) Electrokinetic properties of sepiolite suspensions in different electrolyte media. *J. Colloid Interf. Sci.*, *281*: 240.
15. Swartzen-Allen, S.L.; Matijevic, E. (1974) Surface and colloid chemistry of clays. *Chem. Rev.*, *74*: 385.
16. Saka, E.E.; Güler, C. (2006) The effects of electrolyte concentration, ion species and pH on the zeta potential and electrokinetic charge density of montmorillonite. *Clay Miner.*, *41*: 853.
17. Abate, G.; Masini, J.C. (2005) Influence of pH, ionic strength and humic acid on adsorption of Cd(II) and Pb(II) onto vermiculite. *Colloid Surface A*, *262*: 33.
18. Abate, G.; dos Santos, L.B.O.; Colombo, S.M.; Masini, J.C. (2006) Removal of fulvic acid from aqueous media by adsorption onto modified vermiculite. *Appl. Clay Sci.*, *32*: 261.
19. Dos Santos, A.C.V.; Masini, J.C. (2007) Evaluating the removal of Cd(II), Pb(II) and Cu(II) from a wastewater sample of a coating industry by adsorption onto vermiculite. *Appl. Clay Sci.*, *37*: 167.
20. Da Fonseca, M.G.; de Oliveira, M.M.; Arakaki, L.N.H. (2006) Removal of cadmium, zinc, manganese and chromium cations from aqueous solution by a clay mineral. *J. Hazard. Mater.*, *137*: 288.
21. Abollino, O.; Giacomino, A.; Malandrino, M.; Mentasti, E. (2007) The efficiency of vermiculite as natural sorbent for heavy metals. Application to a contaminated soil. *Water Air Soil Pollut.*, *181*: 149.
22. Ersoy, B.; Çelik, M.S. (2002) Electrokinetic properties of clinoptilolite with mono- and multivalent electrolytes. *Micropor. Mesopor. Mat.*, *55*: 305.
23. Alkan, M.; Demirbaş, Ö.; Doğan, M. (2005) Electrokinetic properties of kaolinite in mono- and multivalent electrolyte solutions. *Micropor. Mesopor. Mat.*, *83*: 51.
24. Kosmulski, M.; Dahlsten, P. (2006) High ionic strength electrokinetics of clay minerals. *Colloid Surface A*, *291*: 212.
25. Doğan, M.; Alkan, M.; Çakir, Ü. (1997) Electrokinetic properties of perlite. *J. Colloid Interf. Sci.*, *192*: 114.
26. Alkan, M.; Karadaş, M.; Doğan, M.; Demirbaş, Ö. (2005) Zeta potentials of perlite samples in various electrolyte and surfactant media. *Colloid Surface A*, *259*: 155.
27. Tsuchida, H.; Ooi, S.; Nakaishi, K.; Adachi, Y. (2005) Effects of pH and ionic strength on electrokinetic properties of imogolite. *Colloid Surface A*, *265*: 131.
28. Niriella, D.; Carnahan, R.P. (2006) Comparison study of zeta potential values of bentonite in salt solutions. *J. Disper. Sci. Technol.*, *27*: 123.

29. Tunç, S.; Duman, O. (2008) The effect of different molecular weight of poly(ethylene glycol) on the electrokinetic and rheological properties of Na-bentonite suspensions. *Colloid Surface A*, *317*: 93.
30. Tunç, S.; Duman, O. (2007) Thermodynamic properties and moisture adsorption isotherms of cottonseed protein isolate and different forms of cottonseed samples. *J. Food Eng.*, *81*: 133.
31. Brunauer, S.; Emmett, P.H.; Teller, E. (1938) Adsorption of gases in multimolecular layers. *J. Am. Chem. Soc.*, *60*: 309.
32. Da Fonseca, M.G.; Wanderley, A.F.; Sousa, K.; Arakaki, L.N.H.; Espinola, J.G.P. (2006) Interaction of aliphatic diamines with vermiculite in aqueous solution. *Appl. Clay Sci.*, *32*: 94.
33. Arab, M.; Bougeard, D.; Smirnov, K.S. (2002) Experimental and computer simulation study of the vibrational spectra of vermiculite. *Phys. Chem. Chem. Phys.*, *4*: 1957.
34. Giese, R.F.; Van Oss, C.J. (2002) Colloid and Surface Properties of Clays and Related Minerals; Marcel Dekker Inc.: New York.
35. Wang, Y.H.; Siu, W.K. (2006) Structure characteristics and mechanical properties of kaolinite soils. I. Surface charges and structural characterizations. *Can. Geotech. J.*, *43*: 587.
36. Shaw, D.J. (1992) Introduction to Colloid and Surface Chemistry, 4th Ed.; Butterworth-Heinemann: New York.
37. Martell, A.E.; Smith, R.M.. (1989) Critical Stability Constants; Plenum Press: New York.
38. Davis, J.A.; James, R.O.; Leckie, J.O. (1978) Surface ionization and complexation at the oxide/water interface. I. Computation of electrical double layer properties in simple electrolytes. *J. Colloid Interf. Sci.*, *63*: 480.